REG-γ associates with and modulates the abundance of nuclear activation-induced deaminase

Yasuhiro Uchimura,[1] Lance F. Barton,[2] Cristina Rada,[1] and Michael S. Neuberger[1]

[1]Medical Research Council Laboratory of Molecular Biology, Cambridge CB2 0QH, UK
[2]Department of Biology, Austin College, Sherman, TX 75090

Activation-induced deaminase (AID) acts on the immunoglobulin loci in activated B lymphocytes to initiate antibody gene diversification. The abundance of AID in the nucleus appears tightly regulated, with most nuclear AID being either degraded or exported back to the cytoplasm. To gain insight into the mechanisms regulating nuclear AID, we screened for proteins interacting specifically with it. We found that REG-γ, a protein implicated in ubiquitin- and ATP-independent protein degradation, interacts in high stoichiometry with overexpressed nuclear AID as well as with endogenous AID in B cells. REG-γ deficiency results in increased AID accumulation and increased immunoglobulin class switching. A stable stoichiometric AID–REG-γ complex can be recapitulated in co-transformed bacteria, and REG-γ accelerates proteasomal degradation of AID in in vitro assays. Thus, REG-γ interacts, likely directly, with nuclear AID and modulates the abundance of this antibody-diversifying but potentially oncogenic enzyme.

CORRESPONDENCE
Michael Neuberger:
msn@mrc-lmb.cam.ac.uk

Abbreviations used: AID, activation-induced deaminase; LMB, leptomycin B; MBP, maltose-binding protein; NES, nuclear export sequence.

Activation-induced deaminase (AID) provides the initial trigger for antibody gene diversification, attacking deoxycytidine residues within the immunoglobulin locus and deaminating them to yield deoxyuridine. The resultant U:G mispairs are then recognized by components of both base excision (uracil-DNA glycosylase) and mismatch repair (MSH2–MSH6) pathways, leading to somatic hypermutation if the deamination occurs within the IgV region, or class-switch recombination if deamination is within the vicinity of the immunoglobulin S regions (Maul and Gearhart, 2010).

As an active DNA mutator, off-target action by AID will predispose to genetic instability; AID is indeed implicated in the causation of several B cell malignancies (Pérez-Durán et al., 2007). There is therefore much interest in the mechanisms that control the level of AID's activity and that direct it toward its natural physiological targets in the immunoglobulin loci (Stavnezer, 2011). In fact, AID is largely found in the cytoplasm. Once imported into the nucleus, some AID localizes to chromatin (including the immunoglobulin loci), where it has been preferentially detected at promoter-proximal pause sites for RNA polymerase II at genes including (though not restricted to) the immunoglobulin loci (Yamane et al., 2011). However, much of the AID imported into the nucleus is likely either rapidly exported back to the cytoplasm by virtue of its carboxy terminal nuclear export sequence (NES; Brar et al., 2004; Ito et al., 2004; McBride et al., 2004) or degraded by the proteasome (Aoufouchi et al., 2008).

Nuclear AID is therefore subject to several possible alternative fates. It could be exported back to the cytoplasm, it could be degraded, or it could be targeted onto chromatin at either the immunoglobulin loci (IgV or switch regions) or elsewhere. These differential fates of nuclear AID are presumably determined by differential interactions in which it partakes. In this paper, with a view to understanding these differential fates, we describe the results of a screen that we have performed to identify proteins interacting specifically with AID within the nucleus.

The Rockefeller University Press $30.00
J. Exp. Med. Vol. 208 No. 12 2385-2391
www.jem.org/cgi/doi/10.1084/jem.20110856

RESULTS AND DISCUSSION

REG-γ associates in high stoichiometry with overexpressed nuclear AID

To facilitate purification of AID-interacting proteins, we used a tagged AID derivative fused at its N terminus to two tandem protein G domains followed by a FLAG3 peptide, with the two protein G domains separated from the FLAG3 peptide by a cleavage site for TEV protease (Fig. 1 A). Most AID in B cells is normally found in the cytoplasm. We therefore used a mutant (F193A), in which the phenylalanine residue within AID's NES had been substituted by alanine, allowing more of the protein to be retained within the nucleus (Fig. 1 B; Geisberger et al., 2009). However, because increased nuclear expression of AID appears to be toxic, we incorporated an additional mutation, a glutamic acid→alanine substitution at AID's active site (E58A), which destroys the enzyme's catalytic activity but does not abolish its ability to coordinate zinc (Fig. S1 A).

Recombinant AID was purified from whole cell extracts of Ramos transfectants that expressed the tagged-nuclear or cytosolic AID (i.e., with or without the F193A NES mutation). The purification procedure comprised binding Protein G–FLAG3-AID onto IgG-Sepharose, releasing the FLAG3-AID by cleavage with TEV protease and then purifying the FLAG3-AID by absorption onto an anti-FLAG mAb matrix and elution with 3xFLAG peptide. After silver staining of a SDS-PAGE gel, the most striking difference between the nuclear and cytosolic AID samples was the presence, specifically in the nuclear sample, of a band of ∼31 kD which was of roughly the same intensity as the putative FLAG3-AID band itself (Fig. 1 C). Mass spectrometric analysis confirmed the identity of the FLAG3-AID band and revealed the 31 kD band to be REG-γ, a nuclear protein (also known as PSME3, PA28γ or 11S regulator) implicated in a pathway of proteasome-dependent but ubiquitin- and ATP-independent protein degradation (Li and Rechsteiner, 2001; Zhou, 2006; Mao et al., 2008). Immunofluorescence analysis confirmed that although the F193A-tagged AID mutant is substantially detected in the nucleus of transfected Ramos cells, wild-type AID and REG-γ are largely found in different intracellular compartments in untransfected Ramos cells with REG-γ appearing exclusively nuclear, whereas AID is largely cytosolic (Fig. 1 B).

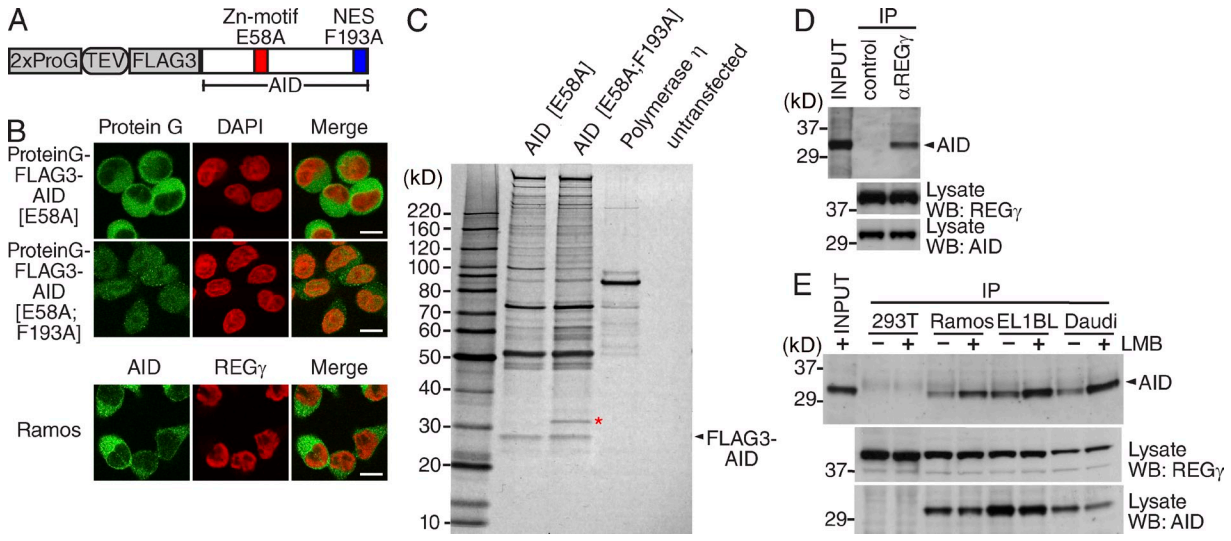

Figure 1. REG-γ co-purifies with tagged and endogenous AID. (A) Schematic depiction of Protein G–FLAG3-AID[E58A, F193A] indicating the Protein G (ProG) domains, TEV cleavage site, and FLAG3-tag epitope linked to a mutated AID, highlighting the Zn coordination motif and NES. (B) Localization in Ramos cells of transfected Protein G–FLAG3-AID[E58A] and Protein G–FLAG3-AID[E58A; F193A] (top two rows) and endogenous AID and endogenous REG-γ (bottom row). Proteins were detected as described in Materials and methods. Nuclei were stained with DAPI. Bars, 10 µm. (C) Silver-stained SDS-PAGE gel of FLAG3-AID purified from Ramos cells transfected with either Protein G–FLAG3-AID[E58A] or Protein G–FLAG3-AID[E58A,F193A]. Parallel purifications from Ramos cells transfected with Protein G–FLAG3-DNA polymerase η and untransfected Ramos cells served as controls. The Protein G–tagged proteins were purified by binding to IgG-Sepharose. After incubation with TEV protease, the eluted FLAG3-AID proteins were further purified by binding to anti-FLAG M2 agarose and eluted with 3xFLAG peptide. After SDS-PAGE and silver staining, mass spectrometric analysis confirmed the identity of the putative FLAG3-AID band (tryptic digested peptides YISDWDLDPGR; AWEGLHENSVR; ILLPLYEVDDLR) and revealed the asterisked band to be REG-γ (LDECEEAFQGTK; SNQQLVDIIEK; MWVQLLIPR; NQYVTLHDMILK). Each lane on the SDS-PAGE gel contains the protein purified from 10^9 Ramos cells. The purifications were repeated in an independent experiment and gave similar results. (D) The presence of AID in anti–REG-γ immunoprecipitates (IP) from lysates of LMB (an inhibitor of Crm1-mediated nuclear export)-treated Ramos cells was analyzed by Western blotting with anti-AID antibody (EK2 5G9). An aliquot (0.4%) of total lysate was loaded as input and aliquots (0.4%) from each total lysate were also probed with anti–REG-γ and anti-AID antibodies. An independent experiment gave similar results. (E) Comparison of the abundance of AID in anti–REG-γ immunoprecipitates from different human B cell lines (Ramos, EL1BL, and Daudi) that had or had not been treated with 20 ng/ml LMB for 4 h before cell lysis. 293T cells served as a negative control. An aliquot (0.2%) of total Ramos lysate was loaded as input and aliquots (0.2%) from each total lysate were also probed with anti–REG-γ and anti-AID antibodies. An independent experiment gave similar results.

REG-γ is associated with endogenous nuclear AID

We were obviously concerned to ascertain whether endogenous (as opposed to overexpressed and tagged) AID is also found to associate with endogenous REG-γ. Immunoprecipitation of REG-γ from Ramos cells does indeed bring down endogenous AID (Fig. 1 D). Furthermore, a larger amount of AID is brought down with immunoprecipitated REG-γ if the Ramos cells are pretreated with leptomycin B (LMB; an inhibitor of Crm1-mediated nuclear export) to increase the concentration of AID in the nucleus (Fig. 1 E). Similar observations were made with two other human B lymphoma lines, EL1BL and Daudi. Because Western blot analysis of separated cytosolic and nuclear fractions shows that ∼10% of the total AID in Ramos cells is associated with the nuclear fraction (unpublished data), we estimate that in the order of ∼5% of the nuclear AID in Ramos cells is brought down by immunoprecipitation with anti-REG-γ antiserum.

Stable direct AID–REG-γ association can be recapitulated in bacteria

We suspected that the interaction between AID and REG-γ might be direct given that REG-γ was brought down in stoichiometric amounts from the Ramos cell transfectants without evidence of other similarly dominant nuclear AID-associated bands (Fig. 1 C). We therefore asked whether we could recapitulate the AID–REG-γ association in bacteria. A fusion protein between AID and maltose-binding protein (MBP; MBP-AID) was coexpressed in *E. coli* with His-tagged REG-γ. Purification of the MBP-AID on an amylose column revealed that the MBP-AID was indeed complexed with His–REG-γ (Fig. 2 A). The extracts of the MBP-AID–expressing bacterial cells also contain a band migrating slightly faster than full-length MBP-AID. Mass spectrometric and N-terminal sequence analyses revealed that this band was caused by truncation of the MBP-AID at AID residue 116. This MBP-AID[116] truncation protein also binds REG-γ, indicating that REG-γ binds residues located within the N-terminal 60% of AID (Fig. 2 B). The binding of MBP-AID to REG-γ appears to be of high affinity with the complex, remaining stable and displaying a constant ratio of MBP-AID to REG-γ through further chromatographic purification (unpublished data).

REG-γ is a member of family of three structurally homologous proteins. REG-α and REG-β are interferon-inducible proteins that function in the cytoplasm, where they form a heteroheptamer which binds to the ends of the core 20S proteasome catalytic machinery and is implicated in peptide generation during the MHC class I pathway of antigen processing (Rechsteiner et al., 2000; Sijts and Kloetzel, 2011). In contrast, REG-γ is nuclear and has been shown to bind a small number of intact proteins, including SRC-3 (steroid receptor co-activator 3; a transcriptional co-activator and oncogene; Li et al., 2006) and cell-cycle regulator p21 (a cyclin-dependent kinase inhibitor; Chen et al., 2007; Li et al., 2007). REG-γ has been implicated in their degradation by a pathway that is both ubiquitin and ATP independent. We found that whereas association is readily detected between MBP-AID and His6–REG-γ coexpressed in *E. coli*, no similar association is seen when MBP-AID is coexpressed with REG-α or REG-β (Fig. 2 C).

Effects of REG-γ on AID abundance and turnover

REG-γ has been proposed to mediate the degradation of both SRC3 and p21 by binding them directly and escorting them to the proteasome (Li et al., 2006, 2007; Chen et al., 2007). To assess whether REG-γ could similarly assist the proteasomal degradation of AID, we asked whether coexpression of REG-γ with tagged AID would lead to accelerated in vitro degradation by purified 20S proteasomes. The results revealed that, in the presence of the proteasome, REG-γ causes substantial destabilization of AID and that this destabilization is inhibited by the protease inhibitor MG132 (Fig. 3 A).

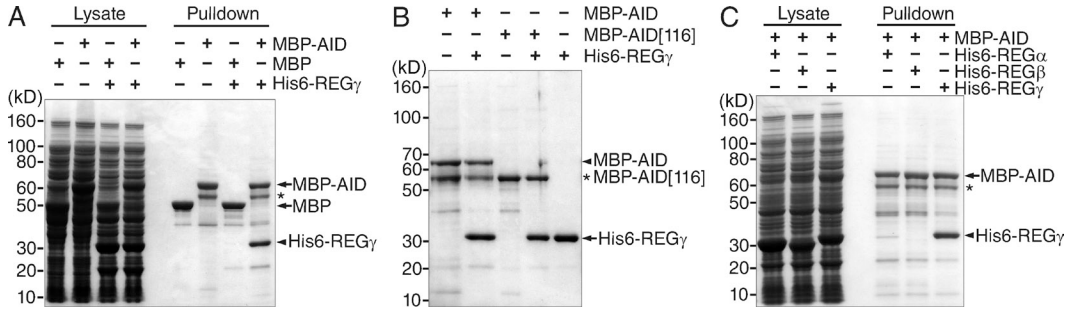

Figure 2. His6–REG-γ interacts directly with MBP-AID. (A) Lysates of MBP- or MBP-AID–expressing *E. coli* cells that had or had not been co-transformed with a plasmid directing expression of His6–REG-γ were analyzed by SDS-PAGE before (left four lanes) and after (right four lanes) pulldown by binding to amylose resin and elution with maltose. The gel (representative of three experiments) was stained with Coomassie blue. The asterisk indicates a truncation product of MBP-AID, which mass spectrometric analysis revealed to be a result of proteolytic cleavage at AID residue 116. (B) Both MBP-AID and MBP-AID[116] form a stable complex with REG-γ. MBPs from lysates of *E. coli* transformants coexpressing MBP-AID[116] and His6–REG-γ (as well as lysates from various control cells) were purified on amylose resin and/or Ni-NTA agarose as appropriate. The gel is representative of three experiments. (C) SDS-PAGE analysis of proteins pulled down on amylose resin from lysates of MBP-AID–expressing *E. coli* cells that had been co-transformed with plasmids encoding His6-tagged REG-α, REG-β, or REG-γ (right three lanes). Whole cell lysates before purification are shown for comparison (left three lanes).

If REG-γ plays a role in the turnover of nuclear AID in normal B cells in vivo, one might expect an increased abundance of AID in its absence. Two groups have described REG-γ–deficient mice and found that they display a very mild phenotype exhibiting a slight growth retardation in one study (Murata et al., 1999) and a small reduction in CD8 T cell numbers in the other (Barton et al., 2004). In most respects, however, the mice resembled their wild-type siblings. To ascertain whether REG-γ deficiency affects AID abundance, we compared AID levels by Western blot analysis in whole cell extracts of (IL4+LPS)-activated splenic B cells from REG-$\gamma^{+/+}$, REG-$\gamma^{+/-}$, and REG-$\gamma^{-/-}$ siblings generated by interbreeding of REG-$\gamma^{+/-}$ heterozygous mice. The results (Fig. 3 B) revealed that B cells from REG-$\gamma^{-/-}$ animals had a significantly higher abundance of AID than their REG-γ–proficient siblings.

Treatment of (IL-4+LPS)-activated B cells with LMB to inhibit AID nuclear export does indeed lead to AID destabilization (Fig. 3 C). This destabilization of AID is somewhat less rapid in REG-γ–deficient B cells, supporting the proposal that REG-γ plays a role in nuclear AID turnover in vivo. However, even in the absence of REG-γ, LMB treatment still leads to rapid AID degradation, indicating that there must also be a REG-γ–independent pathway of destabilization of nuclear AID. Indeed, enforced expression of AID[F193A] mutants in REG-γ–proficient and –deficient B cells revealed that the REG-γ–independent pathway for degrading overexpressed nuclear AID is dependent on AID's lysine residues (Fig. 3 D), consistent with previous evidence of a ubiquitin-dependent pathway of AID turnover (Aoufouchi et al., 2008).

B cells from REG-γ–deficient mice give increased class switching

The efficiency of immunoglobulin class-switch recombination is highly sensitive to the precise abundance of AID. Thus, B cells from AID$^{+/-}$ heterozygous mice exhibit a twofold reduction in class switching (Sernández et al., 2008), whereas increased switching is evident in B cells in which AID expression is up-regulated by freeing it from micro-RNA regulation (de Yébenes et al., 2008; Dorsett et al., 2008; Teng et al., 2008). We were therefore interested to find out whether the increased AID abundance evident in REG-γ–deficient mice correlates with increased class switching.

Culturing splenic B cells from REG-γ–deficient mice in the presence of IL-4+LPS revealed that they exhibited

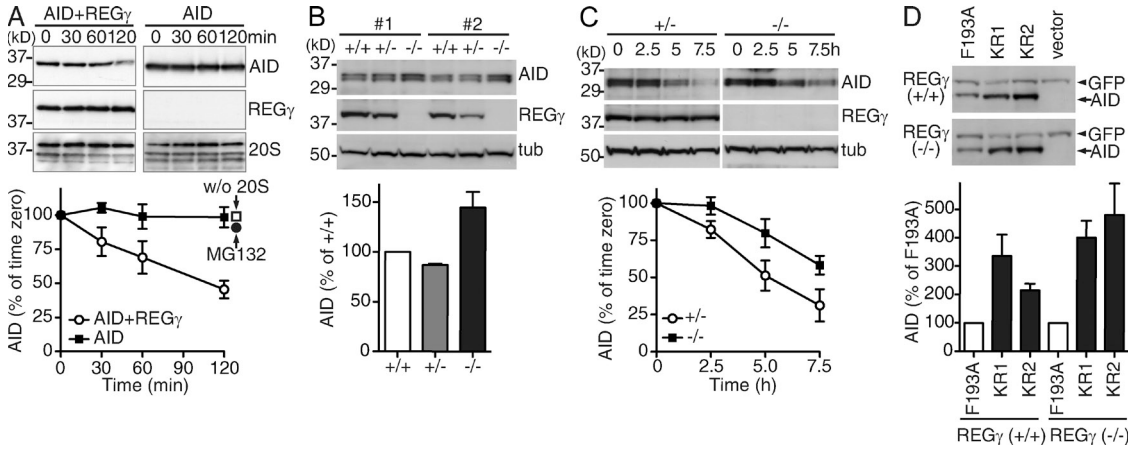

Figure 3. REG-γ is implicated in AID degradation. (A) Lysates of *E. coli* cells that had been induced with IPTG to coexpress His6-AID together with REG-γ (left) or alone (right) were mixed with 20S proteasomes and incubated with 37°C for the indicated times before subjecting to SDS-PAGE. The blots were then probed with anti-AID (EK2 5G9), anti–REG-γ, and anti-20S proteasome antibodies (top). A graph below summarizes the results of two independent such experiments along with controls showing the effects of the inclusion of a proteasome inhibitor (MG132; closed circle) or omission of the 20S proteasome (w/o 20S; open square). Error bars indicate mean ± SEM. (B) 100-µg extracts of purified splenic B cells from REG-$\gamma^{+/+}$, REG-$\gamma^{+/-}$, and REG-$\gamma^{-/-}$ siblings that had been activated for 3 d with IL-4 and LPS were subjected to SDS-PAGE and probed after blotting with anti–mouse AID (mAb 94.16), anti–REG-γ, and anti–α-tubulin (tub) antibodies. Two independent experiments (#1 and 2) are shown in the top, with the results of four independent experiments comparing AID protein abundance in B cells from REG-γ–deficient mice relative to littermates presented in the histogram below. The strengths of the AID bands have been quantified with ImageJ (National Institutes of Health) and normalized with respect to α-tubulin. Error bars indicate mean ± SEM. (C) Purified splenic B cells from REG-$\gamma^{+/-}$ and REG-$\gamma^{-/-}$ siblings were activated for 3 d with IL-4 and LPS and then cultured with 20 ng/ml LMB for 2.5, 5, and 7.5 h. 100 µg LMB-treated extracts was loaded onto SDS-PAGE gels and blots probed with anti–mouse AID, anti–REG-γ, and anti–α-tubulin antibodies (top). Relative AID protein level was quantified with ImageJ and normalized with respect to α-tubulin in each time point. To compare the reduction of AID protein between two genotypes, the level of AID protein at time zero was set to 100%. Pooled data from four independent experiments are plotted below. Error bars indicate mean ± SEM. (D) C-terminally HA-tagged AID[F193A] and two derivatives (KR1 and KR2) in which all eight AID lysine residues had been mutated to arginine (the two derivatives differ in assigned codon usage) were expressed in splenic B cells from REG-$\gamma^{+/+}$ and REG-$\gamma^{-/-}$ mice by retroviral transduction using pMX-IRES-GFP vector. The abundance of AID-HA and GFP in the whole cell extracts 2 d after transduction was monitored by Western blotting (top). The graph below summarizes the results of two independent experiments (all AID mutants analyzed carry the F193A mutation). Error bars indicate mean ± SEM.

substantially increased class switching as compared with their littermate controls in each of six independent comparisons; the mean percentage of $IgG1^+$ cells at day 3 of culture increased from 19.6% in REG-$\gamma^{+/-}$ heterozygous mice to 28.1% in REG-γ–deficient siblings (Fig. 4 A). On average, the REG-γ–deficient B cells gave 40% more switching on day 3 as compared with their litter-matched controls. However, deficiency in REG-γ does not lead to any detectable change in the abundance of γ1-sterile transcripts (Fig. S2 A). Extending the analysis of switching to a further seven sets of litter-matched siblings revealed that although deficiency in REG-γ does not lead to any detectable change in the rate of B cell proliferation, the REG-γ–deficient B cells exhibited a substantially higher proportion of $IgG1^+$ cells compared with the REG-γ–proficient controls as analyzed at each cell division (Fig. 4 B). Furthermore, flow cytometric comparison of bone marrow and spleen samples from REG-$\gamma^{-/-}$ and control siblings did not reveal any changes in B cell development, although it confirmed the previously noted (Barton et al., 2004) very small reduction in the proportion of $CD8^+$ single positive splenic T cells (Fig. S2 C).

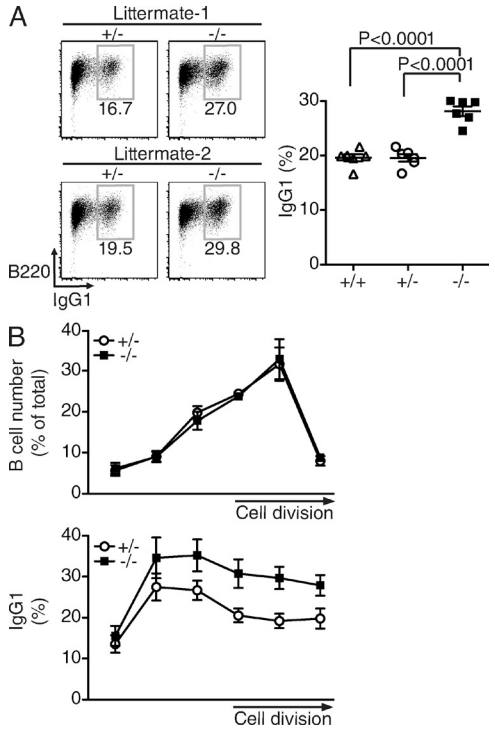

Figure 4. Increased class-switch recombination in B cells from REG-γ–deficient mice. (A) Flow cytometric analysis of class switching in (IL-4+LPS)-activated splenic B cells from REG-$\gamma^{+/+}$, REG-$\gamma^{+/-}$, and REG-$\gamma^{-/-}$ mice. After 3 d of activation, purified splenic B cells were stained with PE-conjugated anti-B220 and biotinylated anti-IgG1, followed by APC-conjugated streptavidin. FACS profiles from two pairs of REG-$\gamma^{+/-}$ and REG-$\gamma^{-/-}$ littermates are shown on the left. A graph on the right summarizes the results from six sets of littermates (error bars indicate mean ± SEM). The p-values were calculated using the unpaired two-tailed Student's *t* test. (B) Purified splenic B cells from REG-$\gamma^{+/-}$ and REG-$\gamma^{-/-}$ mice were labeled with CFSE and stimulated with IL-4 and LPS. After 3 d of activation, the B cells were stained for B220 and IgG1. The graph on the top shows the distribution of the total B cell population on day 3 according to the extent of division they have undergone during culture and the graph below shows the percentage of B cells that have switched to IgG1 at day 3 as a function of the number of cell divisions undergone. A total of seven litter-matched pairs of mice in three independent experiments were analyzed. Error bars indicate mean ± SEM. Representative examples of the primary analyses are shown in Fig. S2 B.

Reduced AID degradation in REG-$\gamma^{-/-}$ mice might also be expected to lead to a more general increase in genomic instability. However, REG-$\gamma^{-/-}$ mice on a normal background do not show any marked increase in tumor incidence, possibly reflecting p53 and other checkpoints (Jankovic et al., 2010). Only a small increase in the frequency of c-*myc*–IgH translocations was detected in cultured B cells from REG-γ–deficient (as opposed to REG-γ–proficient) mice in which AID overexpression had been induced by retroviral transduction (Fig. S3), possibly reflecting the ubiquitin-dependent degradation of such overexpressed AID (Fig. 3 D). Thus, although the results suggest that the dramatically increased class-switching in REG-γ–deficient mice is likely to be at least in part a direct consequence of the increased AID abundance, we cannot exclude the possibility that there is an additional contribution from some as yet unidentified effect of REG-γ deficiency (e.g., a perturbation of AID's interaction with other nuclear partners).

These results identify AID as a novel target of REG-γ regulation. A feature shared by AID with most cellular REG-γ targets identified so far (SRC3, p21, and MDM2-p53; Li et al., 2006, 2007; Chen et al., 2007; Zhang and Zhang, 2008) is that misexpression of these nuclear proteins is potentially oncogenic. With AID, as with the other REG-γ targets, REG-γ contributes to its nuclear degradation but clearly does not provide the sole route to its regulated turnover. Nevertheless, the phenotype of B cells from REG-γ–deficient mice suggests that, under normal conditions, REG-γ might well provide a major pathway of nuclear AID destruction, with other pathways taking over in its absence. It is also possible that the ubiquitin- and ATP-independent REG-γ pathway might prove of especial importance under certain conditions, for example in cells with low concentrations of ATP.

Our results show that ∼5% of the endogenous nuclear AID in Ramos B cells (as well as a substantially higher proportion of overexpressed mutant AID) is associated with REG-γ. Although the structural basis is at present unclear, the bacterial coexpression assays indicate that this interaction is likely direct. We suspect that part of the AID surface might exhibit a naturally unfolded conformation that can fold to adopt a structure, which facilitates interaction with REG-γ or other suitable partners. Indeed, a role for such naturally unfolded segments in REG-γ's clients has already been proposed to account for the ability of REG-γ to mediate the proteasomal degradation of these clients without requirement of ATP (Li and Rechsteiner, 2001; Zhou, 2006). In which case, the ability to interact with REG-γ in vitro might extend to other members of the AID/APOBEC family. We therefore

performed additional bacterial pulldown experiments and found that, although REG-γ exhibits preferential binding to AID, lesser binding is also obtained with APOBEC1 and APOBEC3 when coexpressed in *Escherichia coli* but not with APOBEC2 or substantial amounts of endogenous bacterial proteins (Fig. S1 B). We have been unable to reconstitute the REG-γ interaction with fully denatured MBP-AID, but REG-γ recognition of AID does not require the intactness of AID's Zn-binding motif (Fig. S1 C), although we do not know the effect on AID folding of the loss of critical zinc-coordinating residues. The results are therefore consistent with a model in which AID presents a naturally unfolded face (which might contribute to the stickiness and aggregation of the protein as analyzed in vitro) that could also form part of the site of interaction of AID with several of its bona fide cytoplasmic and nuclear partners. Indeed, the role of REG-γ could be to scavenge unattached AID for degradation in situations when it has been jettisoned by one of its nuclear partners. Alternatively, in view of the apparent high affinity of the AID–REG-γ interaction, REG-γ might serve to actually limit the availability of AID to its physiological or even nonphysiological interactors. Insight into these possibilities might be provided by elucidating the structural basis of the AID–REG-γ interaction, comparing to the interactions that AID displays with other bona fide partners.

MATERIALS AND METHODS

Cell lines. Human AID[E58A], AID[E58A; F193A], and DNA polymerase η cDNAs were cloned into plasmid pEAK8-ProteinG-FLAG3. The pEAK8 plasmid was obtained from Edge BioSystems. Protein G–FLAG3 is a tag comprising two tandem Protein G domains (Bürckstümmer et al., 2006) and a FLAG3 epitope separated by a TEV cleavage site. These plasmids were transfected into Ramos cells by electroporation. Stably transfected colonies were picked up after 2 wk of selection with puromycin and expanded in RPMI supplemented with 10% FBS, 0.05 mM 2-mercaptoethanol, and 0.3 μg/ml puromycin.

Purification and mass spectrometric analysis of tagged AID from Ramos cells. Transfected Ramos clones (10^9 cells) were lysed in 10 ml buffer A (20 mM Hepes, pH 7.9, 10% glycerol, 150 mM NaCl, 2.5 mM $MgCl_2$, 10 μM $ZnCl_2$, 0.2% Triton X-100, 2 mM DTT, and 2 mM *N*-ethylmaleimide) supplemented with 0.4 mg/ml lysolecithin, 50 μg/ml RNase A, and protease inhibitor cocktail (Roche). Clarified lysates were incubated with 150 μl rabbit IgG-Sepharose 6FF (GE Healthcare) at 4°C for 1 h. The IgG-Sepharose beads were washed with buffer A and incubated with 40 U AcTEV protease (Invitrogen) at 4°C overnight. The protein released as a result of TEV cleavage was incubated with 25 μl anti-FLAG M2-agarose (Sigma-Aldrich) at 4°C for 1 h and eluted with 30 μl 3xFLAG peptide (0.15 μg/μl; Sigma-Aldrich). The samples eluted with 3xFLAG peptide were then subjected to SDS-PAGE and stained with a SilverQuest staining kit (Invitrogen). The indicated bands were excised for tryptic digestion. Mass spectrometric analysis was performed with HCT Ultra II with electron transfer dissociation (Bruker Daltonics). Spectra were analyzed with Scaffold 2 proteome software (Proteome Software Inc.).

Immunofluorescence analysis. Cells were fixed with 4% paraformaldehyde and permeabilized with 0.2% Triton X-100. Untransfected Ramos cells were stained with rat anti-AID mAb (EK2 5G9; Cell Signaling Technology), followed by anti–rat IgG-488 (Invitrogen) and rabbit anti–REG-γ (Biomol), followed by anti-rabbit IgG-568 (Invitrogen). Protein G–FLAG3 stable transfectants were stained with goat anti–rabbit IgG-FITC (Southern Biotech; to detect Protein G–containing fusion proteins). Samples were mounted with DAPI-containing mounting medium (VECTASHIELD; Vector Laboratories) and observed using a Radiance 2100 confocal microscope (Bio-Rad Laboratories) with a Plan Apo 60×/1.40 NA oil immersion lens (Nikon) using LaserSharp 2000 acquisition software (Bio-Rad Laboratories).

Immunoprecipitation and Western blot analysis. For analysis of endogenous AID in B cell lines, cells (which had, if required, been preincubated with 20 ng/ml LMB [LC Laboratories] for 4 h at 37°C) were lysed in buffer A supplemented with 0.4 mg/ml lysolecithin, 50 μg/ml RNase A, 150 U/ml benzonase (Novagen), and protease inhibitor cocktail. Clarified lysates were mixed with anti–REG-γ antibody at 4°C for 30 min and incubated with Protein A–Sepharose (GE Healthcare) at 4°C for 30 min. Beads were then washed with buffer A and subjected to SDS-PAGE.

For analysis of endogenous AID in mouse splenic B cells, clarified lysates prepared from cells lysed by 30 min of incubation on ice in 10 mM Hepes, pH 7.9, 150 mM NaCl, 1% Triton X-100, 0.1% SDS, 0.5% deoxycholate, 150 U/ml benzonase, 0.1 mM PMSF, and protease inhibitor cocktail were subjected to SDS-PAGE (100 μg/lane). Protein concentration in lysates was measured with a BCA protein assay kit (Thermo Fisher Scientific). Human AID and REG-γ were detected in Western blots using the same antibodies used for immunofluorescence, whereas mouse AID was detected with mAb 94.16 (provided by Hans-Martin Jäck, Erlangen, Germany) and α-tubulin is a rabbit antiserum (Abcam). Mutant AIDs containing a C-terminal HA tag were expressed in mouse splenic B cells by retroviral transduction using pMX-IRES-GFP vector as previously described (Geisberger et al., 2009).

Class-switching assays. REG-γ–deficient mice that had been bred onto a C57BL/6 background (Barton et al., 2004) were bred in our animal facility under UK Home Office project license PPL80/2226 against C57BL/6 mice. Heterozygous animals were used to produce age-matched littermates of 8–12 wk for class-switching assays. Splenic B cells that had been enriched by depletion of $CD43^+$ cells using anti-CD43–coupled magnetic beads (Miltenyi Biotec) were seeded in 24-well plates (0.5×10^6 per well) in 1 ml RPMI supplemented with 10% FBS, 0.05 mM 2-mercaptoethanol, 25 ng/ml recombinant mouse IL-4 (R&D Systems), and 40 μg/ml LPS (Sigma-Aldrich). On day 3 of stimulation, B cells were stained with PE-conjugated anti-B220 and biotinylated anti-IgG1 (followed by APC-conjugated streptavidin; all from BD). Flow cytometry was performed using an LSRII (BD), excluding dead cells with propidium iodide and analyzing switching data with FlowJo software (Tree Star). For cell division analysis, isolated splenic B cells were stained with 5 mM CFSE (Invitrogen) and stimulated with IL-4 and LPS as described.

Assaying AID–REG-γ association in bacteria. *E. coli* BL21(DE3) cells that had been transformed with AID/APOBEC cDNAs cloned into pMAL-c2X vector (NEB) and/or N-terminally hexa-His–tagged REG-α/β/γ cDNAs cloned into the p15A origin–containing vector pACYC-T7 (Yasukawa et al., 1995) were induced with 0.3 mM IPTG at 20°C for 16 h. Bacterial pellets were sonicated in buffer B (10 mM Hepes, pH 7.9, 200 mM KCl, 0.1% Triton X-100, and 1 mM DTT) containing 10 μg/ml DNaseI, 10 μg/ml RNaseA, 1 mM PMSF, and protease inhibitor cocktail. Maltose binding proteins were purified from the clarified lysates by binding for 1 h at 4°C on to amylose resin (NEB) and eluted from the washed beads with 50 mM maltose in buffer B.

Assaying proteasomal degradation in vitro. *E. coli* BL21(DE3) was cotransformed with pET30 (Novagen)-His6-AID and either pACYC-T7–REG-γ or unmodified pACYC-T7 control plasmid. Cells were induced with 0.3 mM IPTG at 20°C for 16 h. Bacterial pellets were then sonicated in 50 mM Hepes, pH 7.9, 150 mM NaCl, 10% glycerol, 0.5 mM EDTA, and 1 mM DTT, and clarified lysates were incubated with 140 nM 20S proteasomes (BostonBiochem) at 37°C for the indicated times. MG132 (Sigma-Aldrich), where required, was included at 10 μM.

Online supplemental material. Fig. S1 shows that the E58A and truncation mutants of AID retain the ability to coordinate zinc and that, after

coexpression in *E. coli* as MBP fusion proteins, MBP-AID binds REG-γ more strongly than do various MBP-APOBEC chimeras. Fig. S2 compares the abundance of various lymphoid subpopulations, the amount of (IL-4+LPS)-induced sterile γ1 transcripts, and the degree of switching to IgG1 in REG-$\gamma^{-/-}$ and REG-$\gamma^{+/-}$ mice. Fig. S3 compares c-*myc*-IgH translocations in (IL-4+LPS)-activated splenic B cells from REG-$\gamma^{-/-}$ and REG-$\gamma^{+/-}$ mice. Online supplemental material is available at http://www.jem.org/cgi/content/full/jem.20110856/DC1.

We thank Farida Begum for mass spectrometry, Shona Butler and her team for animal husbandry, and Maria Daly and Fan Zhang for cell sorting. We also thank Anita Chandra, Ben Taylor, and Gareth Williams for advice and Hans-Martin Jäck for the gift of the anti-AID antibody.

Y. Uchimura was in part supported by a fellowship from the Japan Society for the promotion of Science. The work was supported by an institutional block grant from the Medical Research Council.

The authors have no conflicting financial interests.

Submitted: 29 April 2011
Accepted: 3 October 2011

REFERENCES

Aoufouchi, S., A. Faili, C. Zober, O. D'Orlando, S. Weller, J.C. Weill, and C.A. Reynaud. 2008. Proteasomal degradation restricts the nuclear lifespan of AID. *J. Exp. Med.* 205:1357–1368. http://dx.doi.org/10.1084/jem.20070950

Barton, L.F., H.A. Runnels, T.D. Schell, Y. Cho, R. Gibbons, S.S. Tevethia, G.S. Deepe Jr., and J.J. Monaco. 2004. Immune defects in 28-kDa proteasome activator gamma-deficient mice. *J. Immunol.* 172:3948–3954.

Brar, S.S., M. Watson, and M. Diaz. 2004. Activation-induced cytosine deaminase (AID) is actively exported out of the nucleus but retained by the induction of DNA breaks. *J. Biol. Chem.* 279:26395–26401. http://dx.doi.org/10.1074/jbc.M403503200

Bürckstümmer, T., K.L. Bennett, A. Preradovic, G. Schütze, O. Hantschel, G. Superti-Furga, and A. Bauch. 2006. An efficient tandem affinity purification procedure for interaction proteomics in mammalian cells. *Nat. Methods.* 3:1013–1019. http://dx.doi.org/10.1038/nmeth968

Chen, X., L.F. Barton, Y. Chi, B.E. Clurman, and J.M. Roberts. 2007. Ubiquitin-independent degradation of cell-cycle inhibitors by the REGgamma proteasome. *Mol. Cell.* 26:843–852. http://dx.doi.org/10.1016/j.molcel.2007.05.022

de Yébenes, V.G., L. Belver, D.G. Pisano, S. González, A. Villasante, C. Croce, L. He, and A.R. Ramiro. 2008. miR-181b negatively regulates activation-induced cytidine deaminase in B cells. *J. Exp. Med.* 205:2199–2206. http://dx.doi.org/10.1084/jem.20080579

Dorsett, Y., K.M. McBride, M. Jankovic, A. Gazumyan, T.H. Thai, D.F. Robbiani, M. Di Virgilio, B. Reina San-Martin, G. Heidkamp, T.A. Schwickert, et al. 2008. MicroRNA-155 suppresses activation-induced cytidine deaminase-mediated Myc-Igh translocation. *Immunity.* 28:630–638. http://dx.doi.org/10.1016/j.immuni.2008.04.002

Geisberger, R., C. Rada, and M.S. Neuberger. 2009. The stability of AID and its function in class-switching are critically sensitive to the identity of its nuclear-export sequence. *Proc. Natl. Acad. Sci. USA.* 106:6736–6741. http://dx.doi.org/10.1073/pnas.0810808106

Ito, S., H. Nagaoka, R. Shinkura, N. Begum, M. Muramatsu, M. Nakata, and T. Honjo. 2004. Activation-induced cytidine deaminase shuttles between nucleus and cytoplasm like apolipoprotein B mRNA editing catalytic polypeptide 1. *Proc. Natl. Acad. Sci. USA.* 101:1975–1980. http://dx.doi.org/10.1073/pnas.0307335101

Jankovic, M., D.F. Robbiani, Y. Dorsett, T. Eisenreich, Y. Xu, A. Tarakhovsky, A. Nussenzweig, and M.C. Nussenzweig. 2010. Role of the translocation partner in protection against AID-dependent chromosomal translocations. *Proc. Natl. Acad. Sci. USA.* 107:187–192. http://dx.doi.org/10.1073/pnas.0908946107

Li, J., and M. Rechsteiner. 2001. Molecular dissection of the 11S REG (PA28) proteasome activators. *Biochimie.* 83:373–383. http://dx.doi.org/10.1016/S0300-9084(01)01236-6

Li, X., D.M. Lonard, S.Y. Jung, A. Malovannaya, Q. Feng, J. Qin, S.Y. Tsai, M.J. Tsai, and B.W. O'Malley. 2006. The SRC-3/AIB1 coactivator is degraded in a ubiquitin- and ATP-independent manner by the REGgamma proteasome. *Cell.* 124:381–392. http://dx.doi.org/10.1016/j.cell.2005.11.037

Li, X., L. Amazit, W. Long, D.M. Lonard, J.J. Monaco, and B.W. O'Malley. 2007. Ubiquitin- and ATP-independent proteolytic turnover of p21 by the REGgamma-proteasome pathway. *Mol. Cell.* 26:831–842. http://dx.doi.org/10.1016/j.molcel.2007.05.028

Mao, I., J. Liu, X. Li, and H. Luo. 2008. REGgamma, a proteasome activator and beyond? *Cell. Mol. Life Sci.* 65:3971–3980. http://dx.doi.org/10.1007/s00018-008-8291-z

Maul, R.W., and P.J. Gearhart. 2010. AID and somatic hypermutation. *Adv. Immunol.* 105:159–191. http://dx.doi.org/10.1016/S0065-2776(10)05006-6

McBride, K.M., V. Barreto, A.R. Ramiro, P. Stavropoulos, and M.C. Nussenzweig. 2004. Somatic hypermutation is limited by CRM1-dependent nuclear export of activation-induced deaminase. *J. Exp. Med.* 199:1235–1244. http://dx.doi.org/10.1084/jem.20040373

Murata, S., H. Kawahara, S. Tohma, K. Yamamoto, M. Kasahara, Y. Nabeshima, K. Tanaka, and T. Chiba. 1999. Growth retardation in mice lacking the proteasome activator PA28gamma. *J. Biol. Chem.* 274:38211–38215. http://dx.doi.org/10.1074/jbc.274.53.38211

Pérez-Durán, P., V.G. de Yebenes, and A.R. Ramiro. 2007. Oncogenic events triggered by AID, the adverse effect of antibody diversification. *Carcinogenesis.* 28:2427–2433. http://dx.doi.org/10.1093/carcin/bgm201

Rechsteiner, M., C. Realini, and V. Ustrell. 2000. The proteasome activator 11 S REG (PA28) and class I antigen presentation. *Biochem. J.* 345:1–15. http://dx.doi.org/10.1042/0264-6021:3450001

Sernández, I.V., V.G. de Yébenes, Y. Dorsett, and A.R. Ramiro. 2008. Haploinsufficiency of activation-induced deaminase for antibody diversification and chromosome translocations both in vitro and in vivo. *PLoS ONE.* 3:e3927. http://dx.doi.org/10.1371/journal.pone.0003927

Sijts, E.J., and P.M. Kloetzel. 2011. The role of the proteasome in the generation of MHC class I ligands and immune responses. *Cell. Mol. Life Sci.* 68:1491–1502. http://dx.doi.org/10.1007/s00018-011-0657-y

Stavnezer, J. 2011. Complex regulation and function of activation-induced cytidine deaminase. *Trends Immunol.* 32:194–201. http://dx.doi.org/10.1016/j.it.2011.03.003

Teng, G., P. Hakimpour, P. Landgraf, A. Rice, T. Tuschl, R. Casellas, and F.N. Papavasiliou. 2008. MicroRNA-155 is a negative regulator of activation-induced cytidine deaminase. *Immunity.* 28:621–629. http://dx.doi.org/10.1016/j.immuni.2008.03.015

Yamane, A., W. Resch, N. Kuo, S. Kuchen, Z. Li, H.W. Sun, D.F. Robbiani, K. McBride, M.C. Nussenzweig, and R. Casellas. 2011. Deep-sequencing identification of the genomic targets of the cytidine deaminase AID and its cofactor RPA in B lymphocytes. *Nat. Immunol.* 12:62–69. http://dx.doi.org/10.1038/ni.1964

Yasukawa, T., C. Kanei-Ishii, T. Maekawa, J. Fujimoto, T. Yamamoto, and S. Ishii. 1995. Increase of solubility of foreign proteins in Escherichia coli by coproduction of the bacterial thioredoxin. *J. Biol. Chem.* 270:25328–25331. http://dx.doi.org/10.1074/jbc.270.43.25328

Zhang, Z., and R. Zhang. 2008. Proteasome activator PA28 gamma regulates p53 by enhancing its MDM2-mediated degradation. *EMBO J.* 27:852–864. http://dx.doi.org/10.1038/emboj.2008.25

Zhou, P. 2006. REGgamma: a shortcut to destruction. *Cell.* 124:256–257. http://dx.doi.org/10.1016/j.cell.2006.01.003